Performance Lab:
Translational Immunogenomics Lab
Kenneth J. Livak, PhD, Director
Dana-Farber Cancer Institute
1 Jimmy Fund Way, Boston, MA 02115

Table 1. Summary of analytical performance findings for bulk RNA TCRseq

Accuracy	Not defined; no predicate standard
Precision	Not applicable. Every aliquot is a sampling from a vast TCR repertoire. Therefore, there are no identical replicates.
Analytical sensitivity	100 pg PBMC RNA if RIN>7
Analytical specificity including interfering substances	Mapping to TCR is based on sequencing data, so all results are specific for CDR3alpha and CDR3beta
Reportable range	100-75,000 unique CDR3alpha clonotypes and 100-250,000 unique CDR3beta clonotypes
Reference interval (normal range)	Not applicable for TCR calls
Standardization, harmonization, reproducibility, and ruggedness	Lack of contamination of empty wells. For clonotype frequencies $>10^{-4}$, correlation of 0.86-0.99 for replicate samples (see **Table 2** and **Figure 8**)
Quality control and improvement procedures	Expected TCR amplification pattern confirmed by Bioanalyzer analysis of sequencing libraries
Any other performance data	

Materials and Methods. Validation was performed on five PBMC total RNA samples isolated from healthy, normal subjects.

TCR primers and protocol for bulk RNA are reported in Keskin *et al*[1]. Sequencing is performed on the MiSeq. Because this is sequencing of targeted amplification products, the sequencing output of the MiSeq is more than adequate for the complexity of the sequencing library. Sequencing parameters are: 248 nt for read 1, 48 nt for read 2, 8 nt for index 1, 8 nt for index 2.

Figure 1 shows the reaction scheme for amplifying TCR alpha and beta CDR3 segments, adding sample-specific barcodes, and preparing libraries suitable for loading on Illumina sequencers. **Figure 2** shows the workflow for the process.

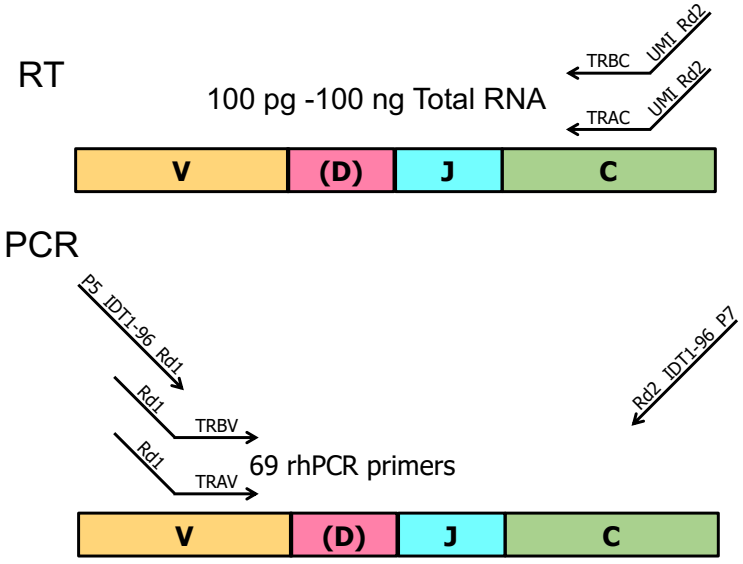

Figure 1. Diagram of DFCI-TIGL method for amplification of TCR CDR3 segments from bulk RNA. This method uses rhPCR technology[2] to improve the specificity for differential amplification of TCR alleles. Inclusion of a single ribo residue in each PCR primer and the use of thermostable RNase H2 in the amplification reaction means that a functional primer is generated only when the oligonucleotide is hybridized to its intended target. In order to avoid the problem of index switching, the method uses double indexing[3].

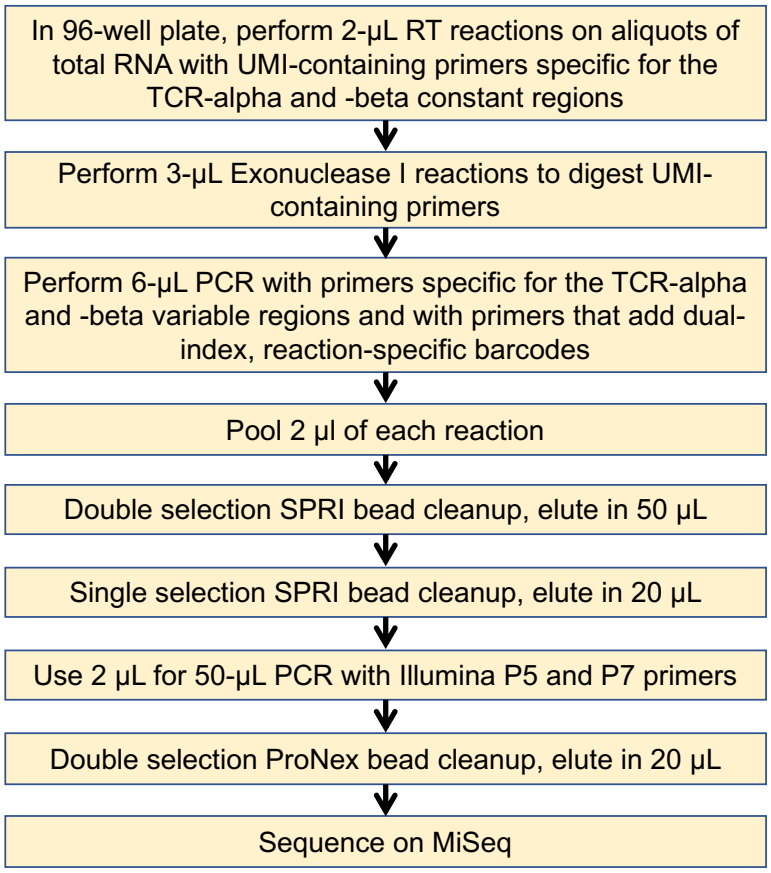

Figure 2. Workflow for DFCI-TIGL method for amplification of TCR CDR3 segments from bulk RNA.

Results

Figures 3-7 show the distribution of alpha and beta clonotypes for the five normal samples. The number of unique clonotypes reported in each panel is the cumulative total across the indicated number of replicates. The assay detects all productive subfamilies reported in the IMGT database. This corresponds to 45 *TRAV* and 53 *TRBV* subfamilies. For the higher input samples (40 ng), a total of 148,618 *TRA* and 432,916 *TRB* unique CDR3 clonotypes were detected across the five subjects.

Comparing the five samples, the number of unique clonotypes detected for the same amount of input RNA can vary up to 8.7-fold. The largest variable affecting clonotypes detected is the fraction of T cells in the original PBMC sample. The next largest variable is the quality of the RNA. We have successfully analyzed RNA with RIN 4 and higher. The variation in T cell fraction and RNA quality make it difficult to specify the read depth required for replicates. For the five samples analyzed here, the average read depths were 32,900 for 10-ng replicates (range 14,200 to 60,800) and 140,400 for 40-ng

replicates (range 30,800 to 305,700). These generated the UMI and unique clonotype results reported in **Table 2**.

Across the five subjects, we observe high correlation (0.86-0.99) in the detection and profiling of *TRB* CDR3 alleles between the lower (10 ng) and higher (40 ng) input samples (**Table 2** and **Figure 8**).

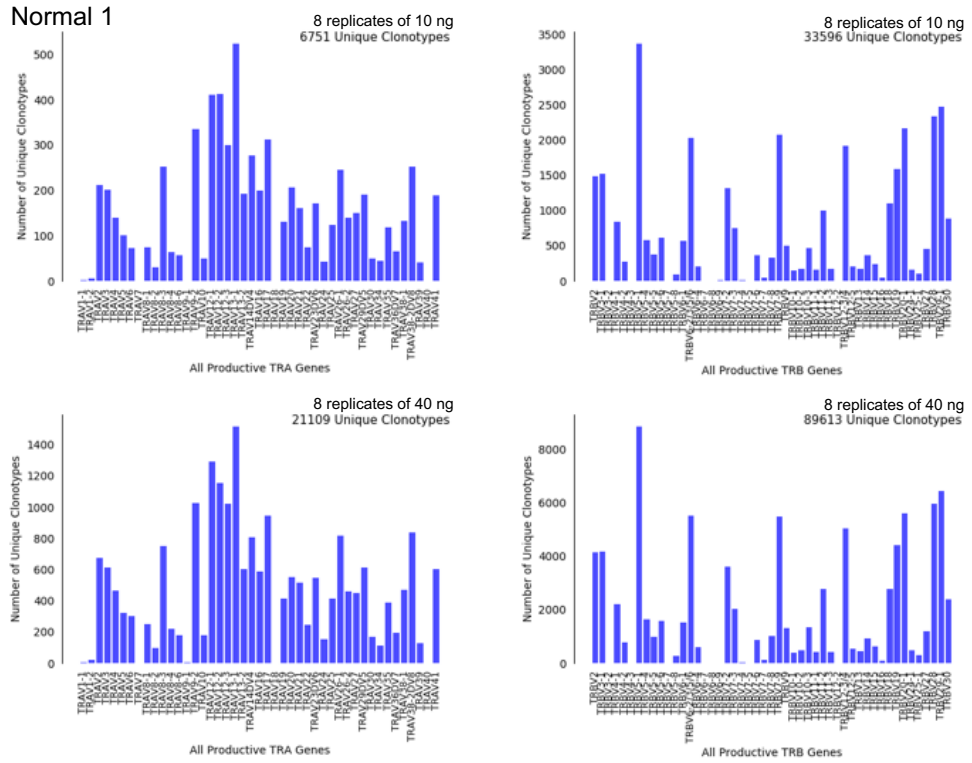

Figure 3. Distribution of unique clonotypes detected for sample 1.

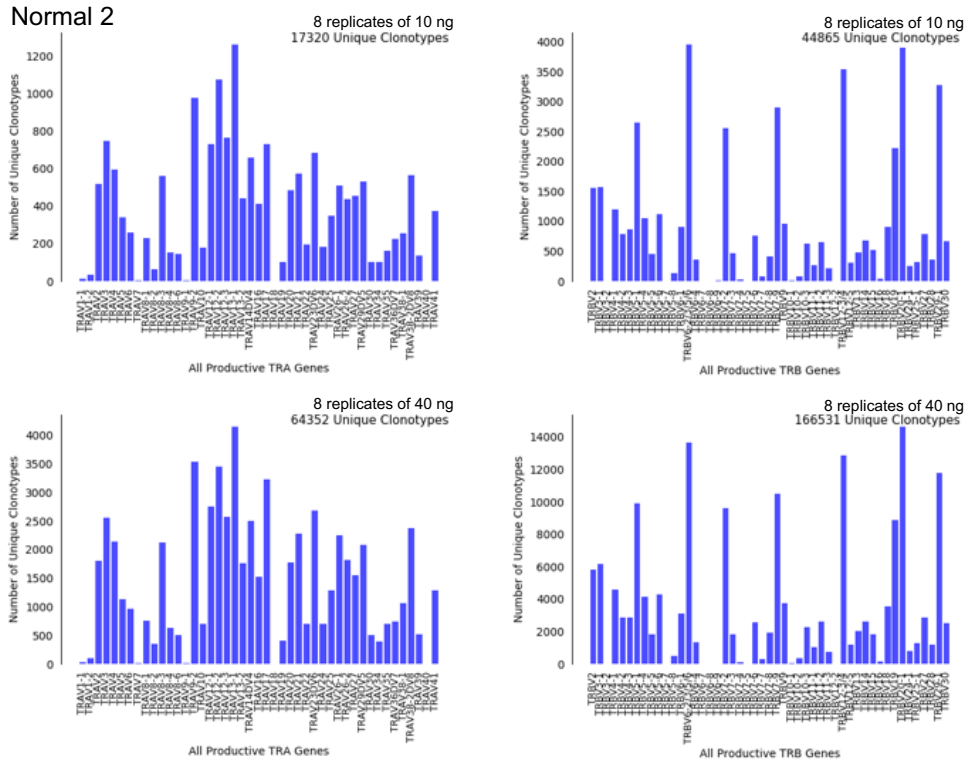

Figure 4. Distribution of unique clonotypes detected for sample 2.

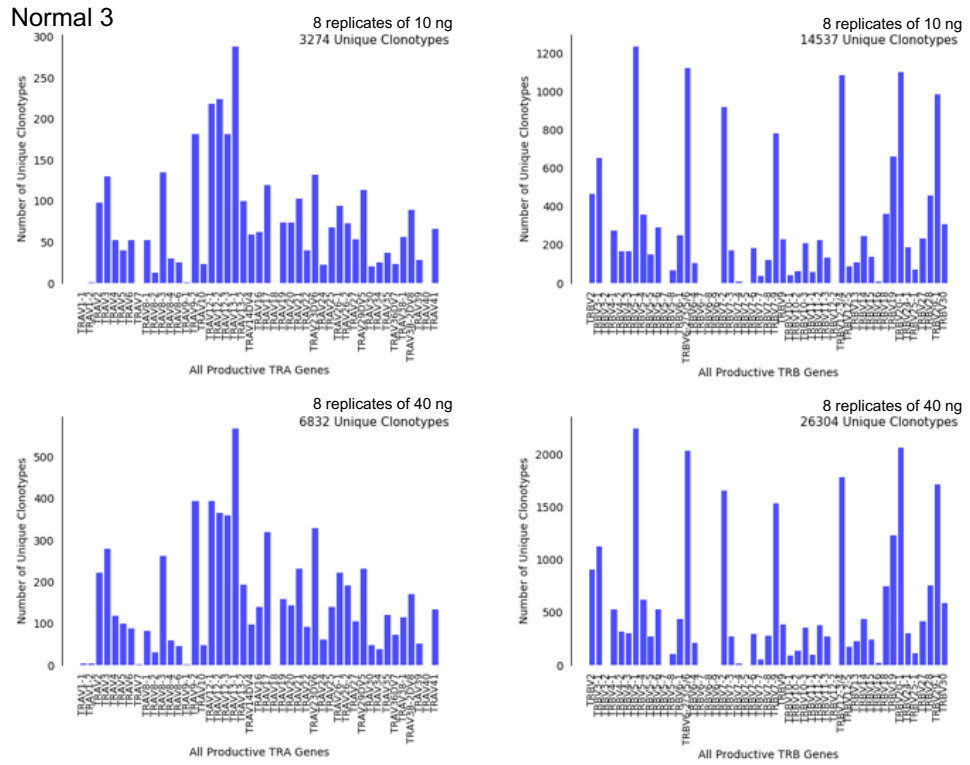

Figure 5. Distribution of unique clonotypes detected for sample 3.

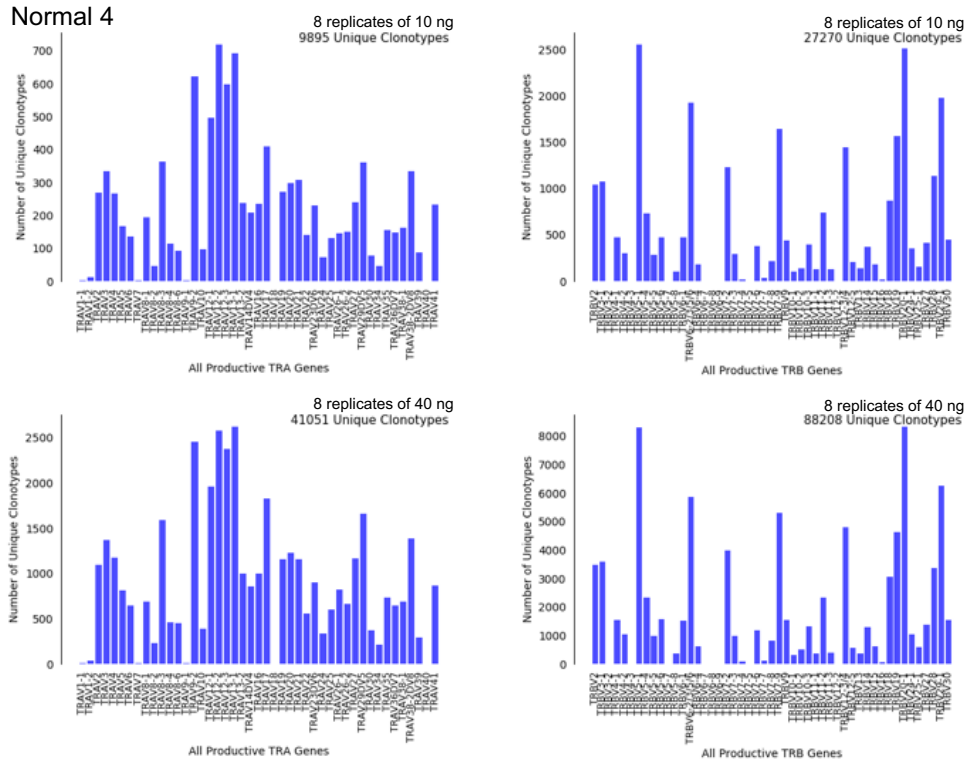

Figure 6. Distribution of unique clonotypes detected for sample 4.

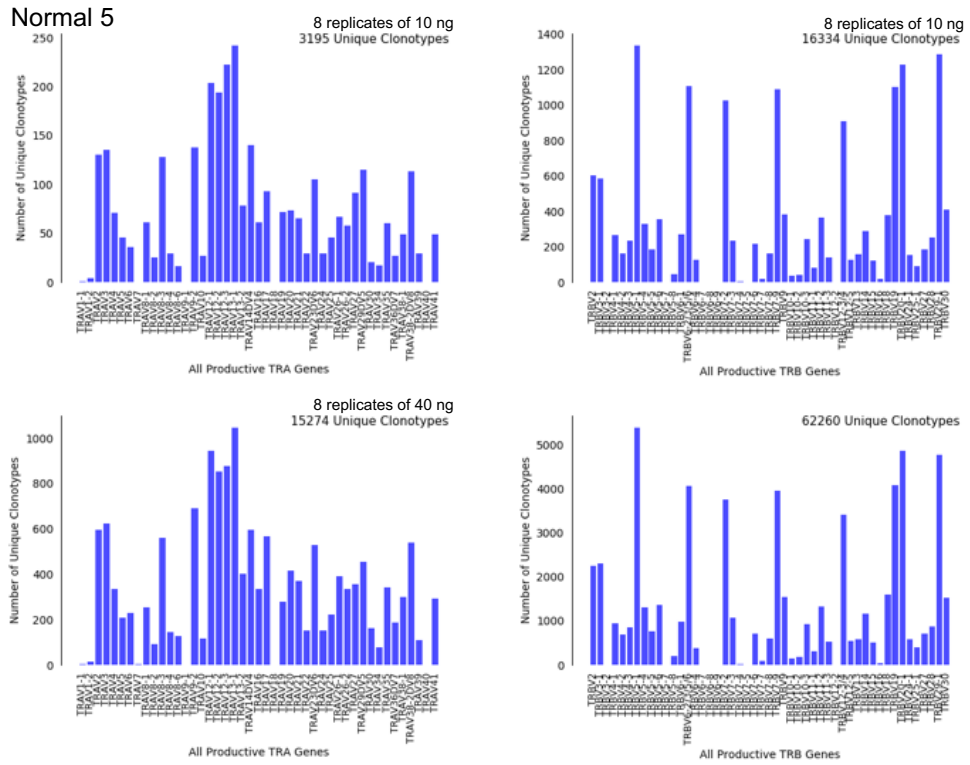

Figure 7. Distribution of unique clonotypes detected for sample 5.

Sample		Replicate size	Average UMI count per replicate	Std dev	Average unique clonotypes per replicate	Std dev	Pearson correlation
1	*TRA*	10 ng	998	145	896	124	0.922
		40 ng	3,951	637	3,311	457	
	TRB	10 ng	5,081	708	4,638	618	0.974
		40 ng	17,025	2,346	14,560	1,868	
2	*TRA*	10 ng	3,128	498	2,511	369	0.980
		40 ng	15,192	2,319	10,092	1,267	
	TRB	10 ng	8,128	1,275	6,459	961	0.996
		40 ng	36,034	3897	25,454	2510	
3	*TRA*	10 ng	488	122	434	100	0.947
		40 ng	1,188	203	1,016	161	
	TRB	10 ng	2,212	382	1,991	334	0.991
		40 ng	4,675	558	4,082	474	
4	*TRA*	10 ng	1,764	514	1,380	361	0.995
		40 ng	9,522	2,974	6,316	1,576	
	TRB	10 ng	5,149	1,131	3,897	828	0.992
		40 ng	19,747	3,968	13,676	2,470	
5	*TRA*	10 ng	478	86	432	77	0.865
		40 ng	2,625	298	2,165	216	
	TRB	10 ng	2645	457	2276	369	0.991
		40 ng	11691	1394	9245	1059	

Table 2. Average UMI counts and number of unique TCR clonotypes detected per 10-ng or 40-ng replicate in five PBMC RNA samples from healthy adult volunteers. The cumulative number of unique TCR clonotypes are reported in **Figures 3-7**. The correlation coefficient is comparing the frequencies for the cumulative results.

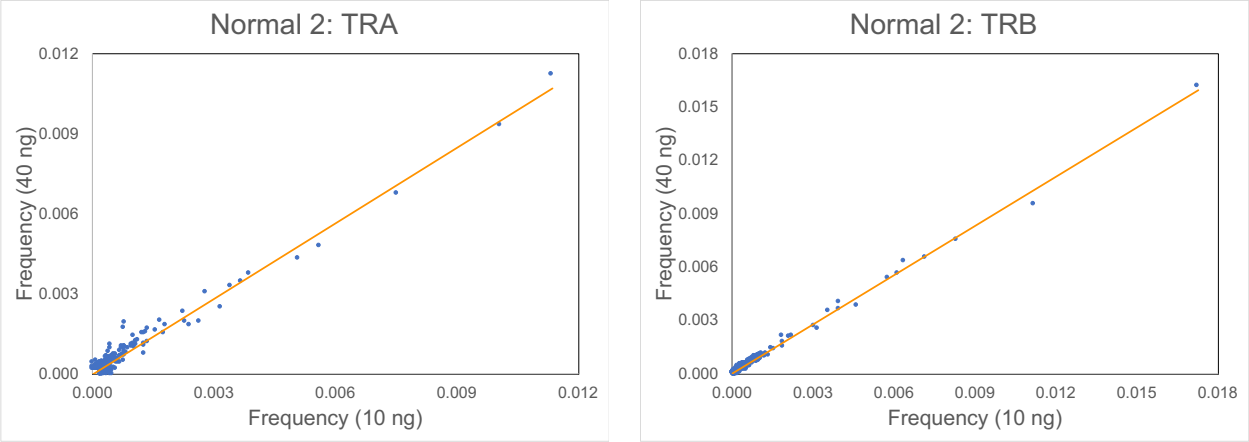

Figure 8. Correlation plot between 10 ng and 40 ng *TRA* (left) and *TRB* (right) cumulative results for sample 2. Correlation coefficients between 10 ng and 40 ng results observed for the five samples are in **Table 2**. In all cases, only frequencies $>10^{-4}$ were compared.

Additional Considerations

When comparing samples, knowing the fraction of T cells aids in the interpretation of TCR frequency data. For blood samples, T cell composition should be obtained by flow cytometry or mass cytometry. Because CyTOF is a Tier 1 CIMAC assay, it is expected that T cell composition will be provided by the CyTOF analysis.

References

1. Keskin, D. B. *et al.* Neoantigen vaccine generates intratumoral T cell responses in phase Ib glioblastoma trial. *Nature* **565,** 234–239 (2019).
2. Dobosy, J. R. *et al.* RNase H-dependent PCR (rhPCR): improved specificity and single nucleotide polymorphism detection using blocked cleavable primers. *BMC Biotechnol.* **11,** 80 (2011).
3. Kircher, M., Sawyer, S. & Meyer, M. Double indexing overcomes inaccuracies in multiplex sequencing on the Illumina platform. *Nucleic Acids Res.* **40,** e3 (2012).